Bethe surface, elastic and inelastic differential cross sections, Compton profile, and binding effects for H_2 obtained by electron scattering with 25 keV incident electrons

R. C. Ulsh, H. F. Wellenstein, and R. A. Bonham

Citation: The Journal of Chemical Physics **60**, 103 (1974); doi: 10.1063/1.1680755
View online: https://doi.org/10.1063/1.1680755
View Table of Contents: http://aip.scitation.org/toc/jcp/60/1
Published by the American Institute of Physics

PHYSICS TODAY
WHITEPAPERS

ADVANCED LIGHT CURE ADHESIVES

Take a closer look at what these environmentally friendly adhesive systems can do

READ NOW

PRESENTED BY
MASTERBOND
ADHESIVES | SEALANTS | COATINGS

Bethe surface, elastic and inelastic differential cross sections, Compton profile, and binding effects for H_2 obtained by electron scattering with 25 keV incident electrons*†

R. C. Ulsh, H. F. Wellenstein, and R. A. Bonham

Department of Chemistry, Indiana University, Bloomington, Indiana 47401
(Received 20 September 1972)

Electron impact spectra for H_2 have been obtained at scattering angles of 1°, 1.5°, 2°, 3°, 4°, 5°, 7°, and 10° using 25 keV incident electrons. The measured intensities were converted to generalized oscillator strengths and placed on an absolute scale at each scattering angle by the use of the Bethe sum rule for the generalized oscillator strength distribution. The cross section differential with respect to both solid angle and energy loss of the scattered electron was corrected for relativistic and exchange effects and integrated over energy loss to obtain the inelastic differential cross sections. In addition the elastic cross section differential with respect to solid angle was measured. The results are all in excellent agreement with theoretical calculations. The total elastic cross section was determined using additional data from another source. The Compton profile was determined from the 7° scattering data and was found to agree well with the previous x-ray results. Consistent generalized optical sums (2,1,−1,−2) and optical sum inequalities for the generalized oscillator strength were also obtained. In addition inelastic scattering factors were computed from the (−1) optical sum and were found to agree well with available theory. Chemical binding effects were explored using electron density difference functions obtained from the differential cross sections. For the first time the intensity difference functions for the elastic and inelastic scattering were determined separately. It is argued that the experimental method used in this study to obtain the intensity difference functions represents the best approach so far developed for obtaining direct information about molecular real space charge densities.

I. INTRODUCTION

In 1930 Bethe[1] established the general theory for inelastic scattering of fast charged particles based on the first Born approximation. Now the theory is well developed relating experimental observables to the electronic structure of atoms and molecules.[2]

The fundamental information which is obtained from scattering experiments relating to the electronic structure of atoms and molecules is the square magnitude of the form factor or equivalently the generalized oscillator strength. The function discussed in this paper is the density of the generalized oscillator strength per unit range of energy loss E defined as[2]

$$df(K,\ E)/dE = \sum_n E_n(|\epsilon_n(K)|^2/K^2)\delta(E_n - E), \qquad (1)$$

where the summation runs over all excited states, discrete as well as continuum,

$$\epsilon_n(K) = \langle \Psi_n | \sum_{j=1}^{N} \exp(i\mathbf{K}\cdot\mathbf{r}_j) | \Psi_0 \rangle$$

is the inelastic-scattering form factor, with Ψ_n and Ψ_0 the total system (atom or molecule) wave functions of the excited and the ground states, respectively, K is the inelastic momentum transfer on collision, and n represents the total set of quantum numbers of the state n. Rydberg atomic units will be used throughout this paper unless indicated otherwise. The generalized oscillator strength per unit range of energy loss E is a very difficult function to evaluate theoretically because accurate eigenfunctions are needed for all ground and excited states of the system. One purpose of this paper is to report the results of experimentally determining the optical oscillator strengths for molecular hydrogen. All experimental studies of the behavior of the generalized oscillator strength with scattering angle to data have been at low energies,[3] small scattering angles,[4] or with insufficient energy resolution.[5] This study encompasses a moderate angular range and relatively high energy (25 keV) where the first Born approximation is likely to be valid.

The characterization of the generalized oscillator strength for a molecule may be illustrated most appropriately in a three dimensional plot of the generalized oscillator strength as a function of energy loss and the natural logarithm of the square of the inelastic momentum transfer, called the Bethe surface,[6] which contains all the information about inelastic charged particle scattering for a particular atom or molecule within the framework of the first Born approximation.

Another important part of the description of the electronic structure of molecules is the determination of the shape of the various charge densities which contribute to the electronic energy. In the case of a diatomic molecule the formation of a bond between two atoms tends to localize the electron densities between the atoms and changes the effective size of the molecule compared to a collection of noninteracting atoms arranged in the same geometrical configuration. The result is usually a decrease of the cross section below that expected for the free atom model. By forming electron density functions for the molecule based on an exact (experimental) electron density and subtracting the contribution from two independent atoms at the same internuclear distance (independent atom model) one obtains a density difference function or Roux function.[7] It has been shown[8] that the

 Copyright © 1974 American Institute of Physics

Fourier transform of this Roux function is closely related to the difference between the elastic differential cross section for the molecule and the one for the independent atom model. Integration of the Fourier transform of the Roux function over all possible values of the momentum transfer yields an approximate energy estimate related to the binding energy of the molecule. A similar analysis applied to the total differential scattering cross section and inelastic differential cross sections separately yields additional energy estimates. The inelastic scattering is connected with the electron-electron exchange energy of the molecular system. The rigorous relationships between molecular energies and scattered intensities are presented in the next section.

II. THEORY

The generalized oscillator strength may be obtained from the experimental cross section differential with respect to scattered solid angle and energy loss through the approximate relation[9]

$$\frac{df(K,E)}{dE} = E\left[\frac{k[K^2(E) - E^2/4c^2]^2(1-\beta^2)}{4k(E)[1-(E/2c^2)(1-\beta^2)^{1/2}]K^2(E)F_{EX}^R}\right] \times\left(\frac{\partial^2\sigma}{\partial\Omega\partial E}\right)_{\text{expt}}, \tag{2}$$

which includes corrections for relativistic and exchange effects where c is the velocity of light, β is the ratio of the incident electron velocity to c, and F_{EX}^R is the correction for exchange given approximately by

$$F_{EX}^R(k, E, \theta) \simeq 1 - \frac{K^2(E) - E^2/4c^2}{[k^4(E) + 4k^2(E)(q^2 - qq' - \Delta/8c^2) + qq'\Delta/c^2 + \Delta^2/16c^4]^{1/2}} + \frac{[K^2(E) - E^2/4c^2]^2[k^2(E) - 2qq' - \Delta/4c^2]}{[k^4(E) + 4k^2(E)(q^2 - qq' - \Delta/8c^2) + qq'\Delta/c^2 + \Delta^2/16c^4]^{3/2}},$$

where E is the energy loss, $K(E)$ is the inelastic momentum transfer, k and $k(E)$ are respectively the relativistic initial and final momenta of the scattered electron, q is given as $(E - K^2)/2K$, q' is $[k(E)k\cos\theta - k^2(E)]/K$, and $\Delta = (E_0 - E)^2$ is the square of the energy of the scattered electron.

The method of placing the experimental cross sections $(d^2\sigma/dEd\Omega)_{\text{expt}}$ on an absolute scale has been discussed previously.[10] The conclusion was that the first Born approximation, the Bethe sum rule, and the corrections outlined in Eq. (2) were valid for the case of 25 keV electrons scattered by He. Since H_2 is similar in many respects to He and since experimental conditions were also very similar it was assumed that the Bethe sum rule

$$S(0, K) = \int dE[df(K, E)/dE] = N \tag{3}$$

could be used to put the double differential cross sections on an absolute scale. Elastic cross sections differential with respect to solid angle can also be obtained in conjunction with the measurements of the inelastic cross sections. Integration of the cross section differential with respect to energy loss and scattered solid angle over energy loss yield the cross section differential with respect to solid angle (referred to here as the differential cross section). In addition the total cross section may be determined by integrating the differential cross section over scattering angle.

Related to the Bethe sum rule, which was used to normalize the data, are certain other useful sum rules. The total Bethe surface can be used to compute sums which are defined as energy moments μ of the generalized oscillator strength, which in this paper will be given as[2]

$$S(\mu, K) = \int E^{\mu}[df(K, E)/dE]\,dE\,. \tag{4}$$

For $\mu = -1$, one obtains the simple formula $S(-1, K) = S(K)/K^2$, where $S(K)$ is the x-ray incoherent scattering factor. Evaluation of $S(0, K)$ yields the Bethe sum rule $S(0, K) = N$ (for any K). There are also other physically meaningful quantities identified with the sum rules.[2] The sum rules provide a powerful control on experimental data and allow consistency checks of the experimental data to be made by use of certain sum rule inequalities.[2]

The Bethe surface also yields information regarding the momentum distribution of target electrons. At large fixed scattering angle it can be shown[9] that a cross section through the Bethe ridge (roughly given by the curve $E = K^2$) provides all the information from which the x-ray Compton profile, written as

$$J(q) = 2\pi \int_q^{\infty} dp\, p\rho(p), \tag{5}$$

can be constructed, provided that the proper relativistic and exchange corrections are made[5,9,11] and the binary encounter theory is valid.

The relationship between the differential cross section and the binding energy of the hydrogen molecule will now be considered in more detail. The potential energy of a molecule can be related to an integration over an expression involving the differential cross section for total scattering (elastic plus inelastic), within the framework of the first Born approximation, as follows. We define a quantity, called a difference function, as the difference between the experimental total differential (elastic plus inelastic) molecular hydrogen cross section and a model molecular differential cross section consisting of the two ground state hydrogen atoms separated by the molecular ground state average internuclear distance (Independent Atom Model, IAM), which can be written as[8]

$$\Delta\left(\frac{d\sigma}{d\Omega}\right)_T = \left(\frac{d\sigma}{d\Omega}\right)_T^{\text{exact}} - \left(\frac{d\sigma}{d\Omega}\right)_T^{\text{IAM}} = \frac{4}{K^4}\left[-2\sum_{n=1}^{N} Z_n\left\langle\int_0^{\infty} dr\, D_n(r) j_0(Kr)\right\rangle_{\text{vib}}\right.$$

$$+\left\langle \int_0^\infty dr\, P(r) j_0(Kr) \right\rangle_{\text{vib}} \Bigg]$$

$$-\frac{4}{K^4}[2(1-F_H)^2[1+\exp(-\langle x^2\rangle K^2/2) j_0(Kr)]$$

$$+2(1-F_H^2)], \tag{6}$$

where $j_0(x)$ is the zero-order spherical Bessel function $\sin x/x$ and Z_n is the atomic number of the nth atom in a molecule containing N atoms. The brackets $\langle\ \rangle_{\text{vib}}$ stand for vibrational average, $\langle x^2\rangle$ is the mean square amplitude of vibration, and F_H is the hydrogen atom x-ray elastic scattering factor. The radial electron densities are defined in terms of the three dimensional one electron charge density and three dimensional electron pair correlation charge density[8] respectively as

$$D_n(r) = r^2 \int d\Omega\, \rho(\mathbf{r}+\mathbf{r}_n) \tag{7}$$

and

$$P(r) = r^2 \int d\Omega \rho c(\mathbf{r}), \tag{8}$$

where $\mathbf{r}_n$ is a vector from the center of mass to the position of the nth nucleus. It is this difference function Eq. (6) multiplied by $K^4/8\pi$ and integrated over all possible values of K which is equal to the chemical binding energy of the molecule provided a small correction for the binding energy of the independent atom model is considered.[8]

The difference function for the elastic differential cross section may be written as[8]

$$\Delta\left(\frac{d\sigma}{d\Omega}\right)_E = \left(\frac{d\sigma}{d\Omega}\right)_E^{\text{exact Born}} - \left(\frac{d\sigma}{d\Omega}\right)_E^{\text{IAM}}$$

$$= \frac{4}{K^4}\Bigg[-2\sum_{n=1}^{N} Z_n \left\langle \int_0^\infty dr\, D_n(r) j_0(Kr) \right\rangle_{\text{vib}}$$

$$+\left\langle \int_0^\infty dr\, E(r) j_0(Kr) \right\rangle_{\text{vib}} \Bigg]$$

$$-[2(1-F_H)^2[1+\exp(-\langle x^2\rangle K^2/2) j_0(Kr)]], \tag{9}$$

where the radial electron density $E(r)$ is defined as

$$E(r) = r^2 \int d\mathbf{r}'\rho(\mathbf{r}') \int d\Omega\, \rho(\mathbf{r}+\mathbf{r}'). \tag{10}$$

Equation (9) yields the difference between the total potential energy of the molecule less the exchange energy and the corresponding energy difference for the IAM model when multiplied by $K^4/8\pi$ and integrated over all K.

It can be seen by inspection of Eqs. (6) and (9) that the expression for the inelastic difference function must be written as

$$\Delta\left(\frac{d\sigma}{d\Omega}\right)_I = \left(\frac{d\sigma}{d\Omega}\right)_I^{\text{exact Born}} - \left(\frac{d\sigma}{d\Omega}\right)_I^{\text{IAM}}$$

$$= \frac{4}{K^4}\Bigg[\left\langle \int_0^\infty dr\, P(r) j_0(Kr) \right\rangle_{\text{vib}}$$

$$-\left\langle \int_0^\infty dr\, E(r) j_0(Kr) \right\rangle_{\text{vib}} \Bigg] - \frac{4}{K^4}[2(1-F_H^2)]. \tag{11}$$

When multiplied by $K^4/8\pi$ and integrated over K Eq. (11) gives the difference between the molecular and IAM exchange energies.[8]

III. EXPERIMENT

The high energy electron spectrometer employed in this study has been described previously[5] except for the insertion between scattering center and detector of an electrostatic differential velocity analyzer of the Möllenstedt type.[12] The chief improvement of this design over the previous one is an increase of the energy resolution from 5 keV to an optimum of 0.4 eV full width half-maximum (FWHM) for 25 keV incident electrons. In addition unwanted background scattering was significantly reduced by use of a double aperture system.

An incident electron beam intensity of up to 100 μA and 400 μ FWHM intersected at right angles a gas jet formed by expansion from a tube with 125 μ inside diameter and 2 mm throat length. The maximum gas beam flow rate was 1.8×10^{20} molecules/sec with a beam divergence angle of about 75°. The pressure of the scattering chamber was found to be proportional to the flow rate with a system pumping rate of 20 000 liters/sec. The scattering chamber background pressure was 3×10^{-7} torr with no target gas present and was allowed to increase to a maximum value of 3×10^{-4} torr during experiments.

At the intersection of the gas and electron beams, about 0.6 to 0.8 mm from the end of the gas nozzle, the divergence of the gas beam and the back diffusion from adjacent surfaces caused background scattering to occur at angles both larger and smaller than the chosen scattering angle. In order to eliminate this type of background scattering a 250 μ width slit system was employed 14 cm from the entrance to the analyzer. By use of identical gas nozzles located in different positions in the scattering chamber it was possible to reproduce the residual gas scattering. Experiments showed that the remaining contribution to the background had essentially the same contour as the spectrum being recorded and was less than 10% at the smallest angle for which measurements were made. A constant background due to random unit scattering and detector noise was also subtracted from the spectra. The magnitude of this correction was obtained from observed counting rates in regions at small and large energy losses where no spectral features were present. In all cases this background was under 0.1% of the maximum value in the inelastic profile. The intensity correction for the finite acceptance angle of the detection system and the finite scattering volume was extensively studied and found to be less than 0.2% for the smallest angles reported in this study.[13]

At a fixed scattering angle, data were collected in a signal averaging mode using 128 channels of a multichannel analyzer which was triggered externally by the voltage ramp driver of the Möllenstedt analyzer. Because the energy loss spectrum was scanned across a detector with a fixed slit geometry it was necessary to divide the total intensity by the scattered electron energy.[14] This correction is less than 2% in the worst case encountered here. For this study the energy resolution of the analyzer was tuned to 3 eV FWHM. The elastic and inelastic spectra were scanned separately under identical experimental conditions. The energy loss scale of the in-

elastic spectrum was calibrated by displaying the elastic peak at fixed intervals across the spectral energy range by applying known bias voltages to the voltage ramp driving the central electrode of the analyzer. The elastic peak was recorded with its energy scale by contracting the scan time scale to obtain greater resolution in the multichannel analyzer (0.2 eV/channel).

The scattering angle was measured using a precision metal film potentiometer with 0.01% linearity directly connected to the center of rotation of the electron gun arm. A voltage with high stability (±0.0005%) was applied across the potentiometer and a ±0.002% digital voltmeter was used to read the ratio of the variable potentiometer voltage to the fixed voltage drop across it. Spectra were recorded at angles of 10°, 7°, 5°, 4°, 3°, 2°, 1.5°, and 1° on one side of 0° and at 1, 4°, 7°, and 10° on the other side. The elastic and total inelastic differential cross sections were obtained by integrating these observed intensities over energy loss at each angle and the zero point was chosen to bring the measurements on the two sides into best agreement. The actual angles were 10.05°, 7.05°, ..., 6.95°, 9.95°. The data were then analyzed as discussed in the next section.

The experiment was designed to comply with three constraints: collection of data in a time short compared to possible experimental fluctuations; low enough count rates to avoid excessive deadtime corrections; and gas flow rates low enough to avoid excessive corrections for multiple intermolecular scattering.

The main source of short term fluctuations was the stability of the electron beam. This problem was solved by the addition of an active feedback filament temperature stabilizing device.[15]

The detection system consisted of a silicon surface barrier detector, preamplifier, spectroscopy amplifier, and multichannel analyzer. It was found that counting rates above about 200 kc caused saturation of the detection system and could not be corrected for. The determination of the system deadtime was done using the peak intensities of elastic and inelastic cross sections at a large fixed scattering angle. The inelastic peak counting rate was always small enough to ensure small deadtime corrections. Study of the variation of the ratio of elastic to inelastic peak intensity values as a function of the incident beam current made it possible to obtain the needed correction. The correction to the counting rate was found to obey the well known relation[16]

$$f_c = f/(1 - f\tau), \tag{12}$$

where f is the measured frequency, f_c is the corrected frequency, and τ is the deadtime which for this experimental setup was found to be $3.05 \pm 0.02 \times 10^{-6}$ sec, corresponding to a correction of 35% at 150 kc. Counting rates for this study were always chosen to be less than 125 kc.

The multiple scattering problem alluded to earlier has been shown to arise from a near zero angle inelastic scattering followed by an elastic scattering at the experimental angle or vice versa. This mechanism was studied in the helium case[10] and found to contribute no significant error at any angle used in this study (i.e., less than a 0.5% correction).

At each scattering angle the product of electron beam current, gas flow rate, and number of scans was adjusted to give cross sections integrated over energy loss with statistical uncertainties less than 1%. Because the inelastic differential cross section increases more than three orders of magnitude going from 10° to 1° it was necessary to decrease the gas flow rate and electron beam current at 7°, 4°, and 1.5° in order to remain under the 125 kc maximum counting rate. At each angle for which the parameters were changed data were taken for both the old and new settings. Duplicate readings at the same angle served as a check on the counting rate correction, the sum rule normalization procedure, and provided a means for obtaining quantitative estimates of the uncertainties in the results.

IV. EXPERIMENTAL RESULTS

Normalization of the experimental generalized oscillator strength by use of the Bethe sum rule $S(0, K) = N$, where N is the total number of electrons in the target system, at each angle produced excellent agreement between theory and experiment in the helium case.[10] Considering this fact and the similarity between the hydrogen and helium experiments it was felt that the sum rules should not fail in this angular range for similar systems and indeed should provide a reliable way to scale the hydrogen data.

In Figs. 1 and 2 the normalized experimental cross section differential with respect to energy loss and scattered solid angle, $(\partial^2\sigma/\partial\Omega\partial E)$, are plotted for all angles studied except 1.5° which was omitted for clarity. The sharp feature on the 1° and 2° curves occurring at ~13 eV energy loss is due to the resonance transition $^1\Sigma_u^+ \leftarrow {}^1\Sigma_g^+$. This portion of the spectrum was examined separately by scanning the energy loss range from 0–100 eV and was later normalized onto the total spectrum. A

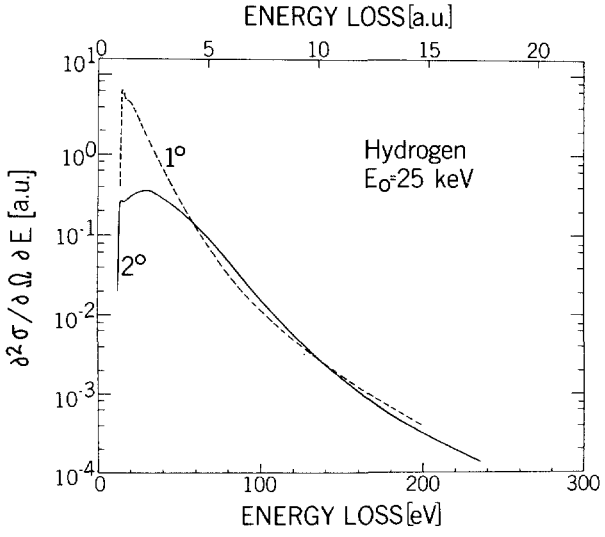


FIG. 1. Experimental cross sections differential with respect to scattered solid angle and energy loss for hydrogen at 1° and 2° scattering angles showing the resonance excitation at ~13 eV and the ionization continuum. Note that the experimental results at 1.5° have been omitted for clarity.

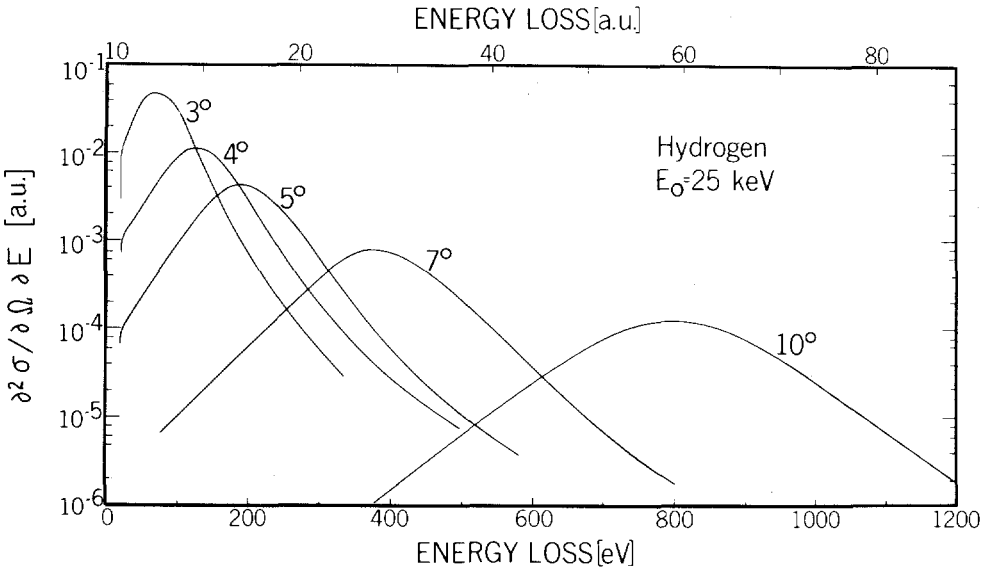


FIG. 2. Experimental cross sections differential with respect to scattered solid angle and energy loss for hydrogen at 3, 4, 5, 7, and 10° scattering angle. By 3° the resonance excitation is too low in intensity to be shown on this graph.

search was also made for two electron transitions between 40 and 45 eV analogous to the $2s2p$ excitation at 60 eV observed in the case of He.[10] No evidence for any transition of this type at 0.1% of the background intensity was observed at any angle. This contrasted to the He case where even at 2.7° the $2s2p$ peak was observed to be $1\frac{1}{2}$% of the background intensity. It can be concluded that the intensity relative to the background of such transitions in H_2 must be at least 15 times smaller than the same intensity ratio in the He case if indeed the transition lies between 40 and 45 eV.

The embodiment of all the inelastic scattering information contained in this study is presented in comprehensive form in the three dimensional plot of the Bethe surface for molecular hydrogen shown in Fig. 3. The generalized oscillator strength is displayed as a function of energy loss and inelastic momentum transfer $[\ln(K)^2]$. By 3° the total contribution to the generalized oscillator strength comes from excitation to the continuum, which

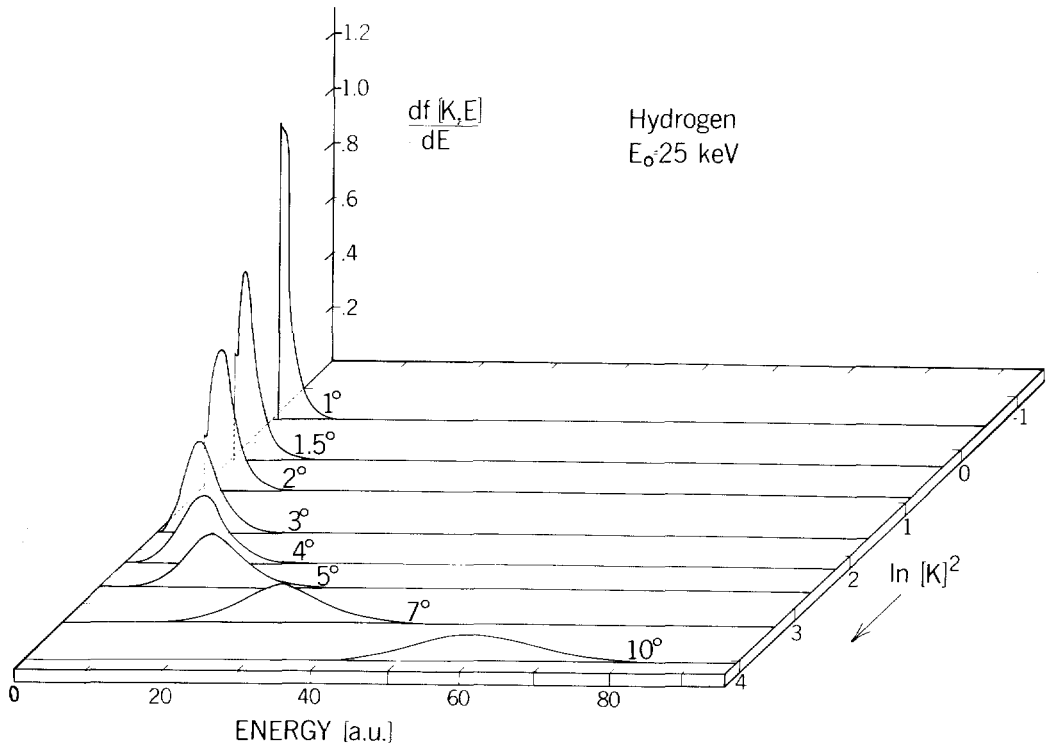


FIG. 3. The Bethe surface for hydrogen with 25 keV incident electrons $df(K, E)/dE$ represents the generalized oscillator strength at a given value of energy loss and momentum transfer.

for the peak of the Bethe ridge can be seen to follow the curve given approximately by $K^2 = E$.

The Compton profile $J(q)$ was extracted from the cross section of the Bethe surface at 5°, 7°, and 10°. Values at the three angles for the Compton profile obtained for the high energy loss side of the inelastic peak were in good agreement. The 7° results were the best values obtained in this work. Shown in Table I is a comparison between the experimental values of this work, those of Eisenberger[17] using x rays, and values calculated by Brown and Smith[18] using a 39 term configuration interaction (CI) wave function. The agreement between the two experimental studies is seen to be excellent. However, since the average agreement in $S(K)$ between theory and experiment is about 2% (see Table IV), there exists an argument that the experimental uncertainties in Table I (which reflect only the error involved in counting statistics) are unreasonably small, and the present disagreement between theory and experiment cannot be regarded as significant.

In Fig. 4 the elastic and inelastic differential cross sections $(d\sigma/d\Omega)_{E,I}$ are plotted against the scattering angle. The estimated experimental uncertainty in these cross sections is too small to be shown on this graph (< 5%). For the elastic case the agreement between experiment

TABLE I. Comparison of experimental and theoretical Compton profiles for molecular hydrogen.

q	H_2—expt.[a] (%)	H_2—expt.[b] (%)	CI—theory[c] (%)
0	1.516 ± 1	1.513 ± 0.7	1.529
0.1	1.488	1.475	1.493
0.2	1.372	1.378	1.393
0.3	1.230	1.240	1.245
0.4	1.050	1.065	1.069
0.5	0.878	0.887	0.888
0.6	0.721 ± 2	0.712 ± 1	0.717
0.7	0.566	0.561	0.566
0.8	0.459	0.435	0.440
0.9	0.355	0.334	0.337
1.0	0.261	0.255	0.257
1.2	0.159 ± 6	0.150 ± 3	0.147
1.4	0.089	0.089	0.034
1.6	0.052	0.051	0.049
1.8	0.030 ± 20	0.030 ± 10	0.029
2.0	0.019	0.015	0.017

[a] Our experiment at 7.05°. Values and uncertainties obtained from overlapping plots of the low and the high energy loss sides of $J(q)$.

[b] X-ray scattering results of Eisenberger.[17]

[c] The calculations of Brown and Smith[18] using a 39 term CI wave function.

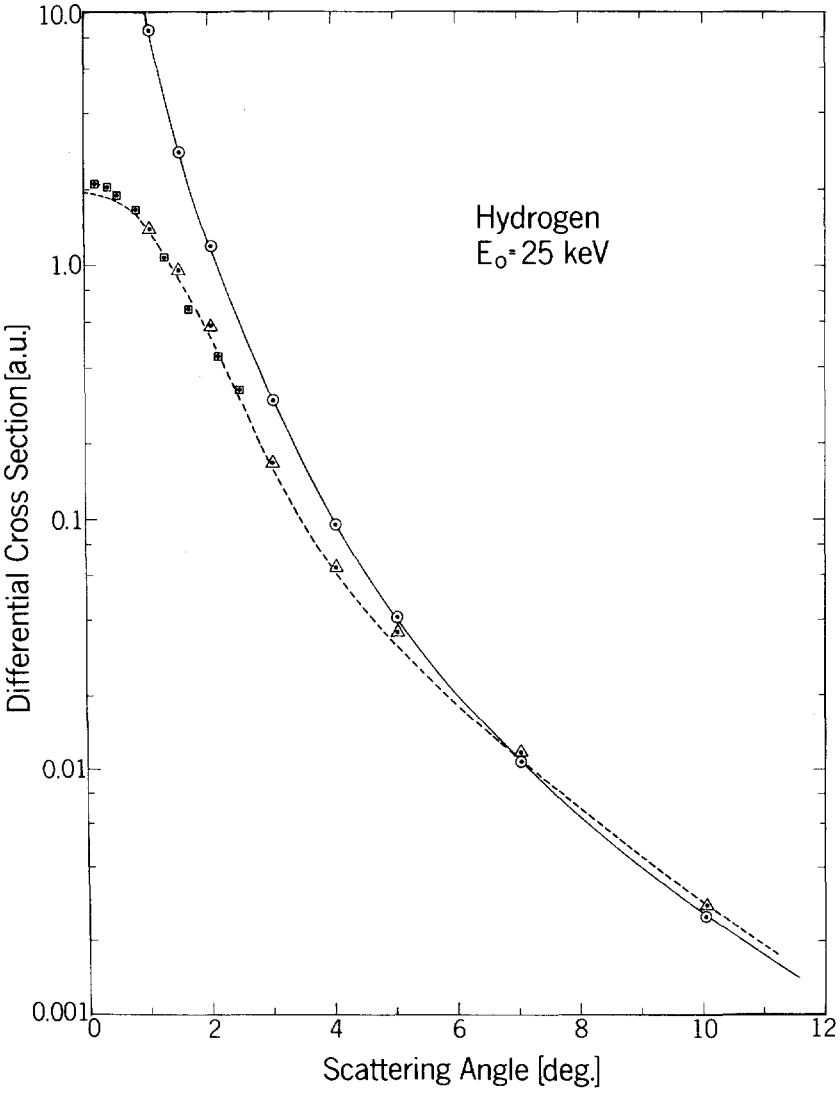


FIG. 4. Cross section differential with respect to scattered solid angle for hydrogen. Symbols refer to experimental quantities as: Δ stands for elastic cross section (this study); ⊡ stands for elastic cross section (Geiger[4]); ⊙ stands for inelastic cross section (this study). The dotted line corresponds to the theoretical elastic cross sections of Brown[19] and Liu.[20] The difference between the two theories are indistinguishable in this plot. The solid line corresponds to the theoretical inelastic cross section of Liu.[20]

and the theory given by Brown[19] and Liu[20] are rather good at small angles. Values for the relative elastic differential cross sections at small angles (< 2.5°) have been given by Geiger[4] and are also shown in Fig. 4, normalized to the cross sections of this study in the region of overlap. Assuming a Rutherford type Coulombic contribution for angles larger than 10° the experimental total elastic cross section was calculated to be $\sigma_T^{expt} = 0.00789 \pm 0.00010$ (a.u.)^2. This value can be compared with that calculated for two hydrogen atoms, $\sigma_T^{2H} = 0.0102$ (a.u.)^2 which is an upper limit on the true total elastic cross section since binding effects reduce the size of the cross section.

The theoretical inelastic differential cross sections shown in Fig. 4 as calculated by Liu[20] from five configuration-interaction (CI) wavefunctions agree well with the experiment. No attempt was made to obtain the total cross section from the inelastic differential cross section because of the limited small angle range of $\ln(K^2)$ used in this study (+4.0 to −0.4).

An examination of the effects of chemical binding on the electron density in scattering space for the hydrogen molecule was carried out in order to observe, for the first time, the separate behavior of the elastic and inelastic contributions to the intensity difference functions. The experimental elastic difference function is plotted in Fig. 5. The corresponding integrated area under the difference function for the elastic cross section is proportional to the difference between the total potential energy of the molecule less the exchange energy and the corresponding energy difference for the IAM model. The experimental uncertainties were determined by comparison of the consistency between duplicate measurements under different, but known, experimental conditions at the same scattering angle and comparisons between results for the same angle in the counter clockwise and clockwise directions. The major contribution to the uncertainty is thought to come from the error in measuring the scattering angle. The big uncertainties at the larger angles and paucity of data made it unreasonable to try to obtain quantitative estimates of molecular energies from this experiment. Also included in Fig. 5 are plots of the difference function obtained from the theoretical elastic differential cross sections given

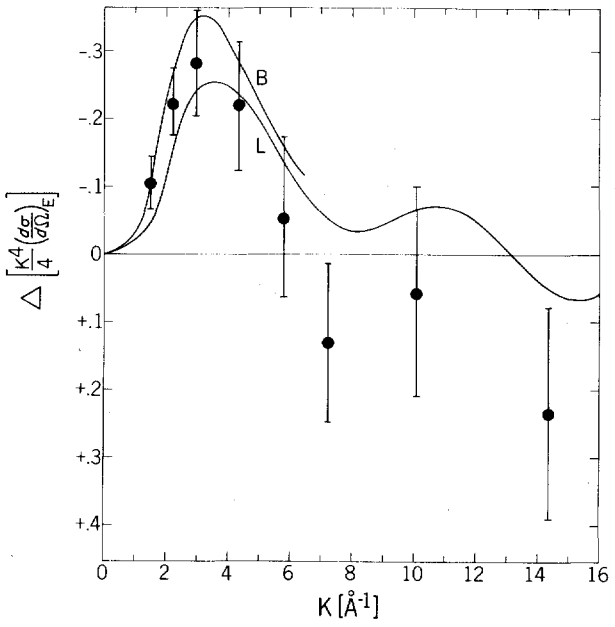


FIG. 5. Elastic difference function for hydrogen. The solid circles correspond to experimental points with the uncertainty indicated by vertical error bars. The solid line marked B is theory given by Brown[19] and the solid line L is theory by Liu.[20] The curve B is preferred because of the superior quality of the wave function used in the calculation and the more rigorous accompanying computational procedures. The area under the curves corresponds to the difference between the total potential energy of the molecule less the exchange energy and the corresponding energy difference for the IAM theory.

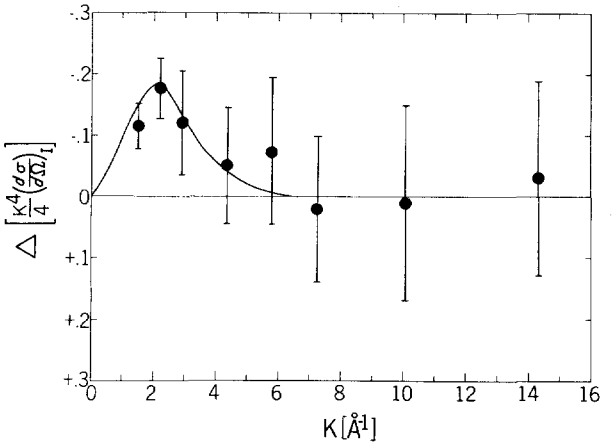


FIG. 6. Inelastic difference function for hydrogen. The solid circles correspond to experimental points with the uncertainty indicated by vertical error bars. The solid line is theory given by Liu.[20] The area under the curves corresponds to the exchange energy difference between the molecule and the IAM theory.

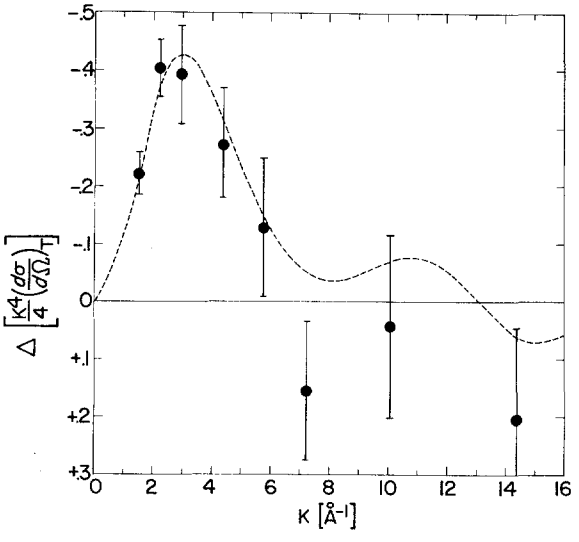


FIG. 7. Total difference function for hydrogen. The solid circles correspond to the sum of the experimental values obtained from Fig. 5 and 6 at constant scattering angle. Note that the uncertainty remains the same as in the previous cases since results for the same angle were obtained under identical conditions. The dotted line is the theory given by Liu.[20] The area under the curves corresponds to the difference between the total potential energy of the molecule and the IAM theory.

TABLE II. Experimental sum rule values for hydrogen using the $S(0, K)$ sum for placing the experimental data on an absolute scale.

Scattering angle (deg.)	K(a.u.)	$S(2,K)$	NK^4 [a]	$S(1, K)$	NK^2 [b]	$S(-1, K)$	NK^{-2} [c]	$S(-2, K)$	NK^{-4} [d]
1	0.7953	13.5±.07	0.800	4.32±.13	1.26	1.21±0.04	3.16	0.892±0.045	5.01
1.5	1.174	25.3±1.0	3.80	5.98±.18	2.70	0.870±0.026	1.45	0.464±0.023	1.05
2	1.552	40.4±4.0	11.6	7.91±.40	4.82	0.650±0.032	0.830	0.273±0.027	0.345
3	2.309	113±11.0	56.8	13.8±.07	10.7	0.351±0.018	0.375	0.0783±0.0078	0.0704
4	3.064	290±14	176	22.5±1.4	18.8	0.203±0.012	0.213	0.0249±0.0030	0.0227
5	3.819	552±66	425	31.8±2.0	29.2	0.138±0.0083	0.137	0.0109±0.0013	9.40×10^{-3}
7	5.325	1870±280	1608	59.7±4.8	56.7	0.0705±0.0056	0.0705	$(2.65\pm0.4)\times10^{-3}$	2.49×10^{-3}
10	7.572	7430±1100	6574	121.±9.7	114.7	0.0341±0.0027	0.0349	$(6.02\pm0.9)\times10^{-4}$	6.08×10^{-4}

[a] $\lim K\to\infty$, $S(2, K)\to NK^4$.
[b] $\lim K\to\infty$, $S(1, K)\to NK^2$.
[c] $\lim K\to\infty$, $S(-1, K)\to N/K^2$.
[d] $\lim K\to\infty$, $S(-2, K)\to N/K^4$ (see discussion in Ref. 10).

by Brown (B)[19] and Liu (L).[20] These difference curves show in a rather direct way how molecular binding energy contributions are spatially distributed. Note that the most important contribution to the difference curve and hence binding energy comes at small values of K. Since small values of K correspond to scattering from the outer or valence shell electrons this observation is not surprising.

The total inelastic scattering can be analyzed in the same manner and the area of the resulting difference function can be shown to yield the difference between the molecular and IAM exchange energies. The results are shown in Fig. 6. Again the agreement between theory[20] and experiment is excellent.

In Fig. 7 the experimental total difference function has been obtained by summing the elastic and inelastic difference functions. The integral over momentum transfer for this case is proportional to the total potential energy of the molecule minus the total potential energy of the IAM model. The results are in agreement with the theory as given by Liu[20] for a vibrationally averaged cross section and the previous experimental results of Kohl and Bonham[21] and Iijima and Bonham.[22] These latter results are not shown in Fig. 7 for clarity but are essentially identical to the present experimental values for $2\leq K\leq 6$ a.u.

In addition to the differential cross sections the sums over the generalized oscillator strengths $S(\mu, K)$ were calculated for $\mu=-2, -1, +1, +2$. The results for these sums are given in Table II. Estimates of the uncertainties were obtained by comparing the sums from both sides of the zero angle for the scattering angles 1°, 4°, 7°, and 10°, and by comparing the sums at high counting rates and low counting rates at fixed angle for the angles 1.5°, 4°, and 7°. As a measure of the reasonableness of these sums the following checks were made. The inequality $S^2(\mu, K)\leq S(\mu-\nu, K)S(\mu+\nu, K)$ (for any real ν) was computed for ($\mu=0$, $\nu=1$, 2), ($\mu=1$, $\mu=1$) and ($\mu=-1$, $\nu=-1$) at all experimental angles. The inequalities were found to hold in all cases and are shown in Table III.

Making use of the relation $S(-1, K)=S(K)/K^2$, where $S(K)$ is the x-ray incoherent scattering factor, the experimental values for $S(K)$ were obtained and are compared in Table IV with the vibrationally averaged theoretical values of Liu which were also used to calculate the inelastic differential cross sections shown in Fig. 4 and the theoretical inelastic difference function shown in Fig. 6. The scatter of the $S(K)$ values for the largest three angles from the theoretical value of 2 may be taken as additional confirmation of the uncertainties plotted in Figs. 5–7. The agreement between theory and experiment for the inelastic scattering factors is less than the estimated experimental uncertainties except at the smallest angle studied.

In this work no serious systematic disagreements between theory and experiment were found for any facet of the Bethe surface examined. Thus the first Born theory of inelastic scattering has been substantiated for numerous properties of the H_2 Bethe surface. This agreement suggests that the keV electron scattering technique may be successfully applied to obtain reliable Bethe surfaces for simple diatomic molecules as well as the

TABLE III. Experimental sum rule inequalities for molecular hydrogen.

Scattering angle (deg.)	K(a.u.)	$S^2(0, K)\leq S(-1, K)S(1, K)$	$S^2(0, K)\leq S(-2, K)S(2, K)$	$S^2(1, K)\leq S(0, K)S(2, K)$	$S^2(-1, K)\leq S(-2, K)S(0, K)$
1	0.7953	4<5.2	4<12.0	18.7<37	1.46<1.8
1.5	1.174	4<5.2	4<11.7	35<51	0.75<0.92
2	1.552	4<5.1	4<11	62<81	0.42<0.52
3	2.309	4<4.8	4<5.8	190<126	0.12<0.16
4	3.066	4<4.6	4<7.2	506<580	0.04<0.05
5	3.823	4<4.4	4<6.05	1011<1100	0.019<0.022
7	5.334	4<4.2	4<4.95	3136<3600	0.0050<0.0054
10	7.599	4<4.14	4<4.44	14600<14800	0.00116<0.00120

TABLE IV. Experimental and theoretical x-ray incoherent scattering factors for hydrogen.

Scattering angle (deg.)	K(a.u.)	$K^2S(-1, K)$ $\langle S(K)\rangle_{vib}^{EXPT}$	$\langle S(K)\rangle_{vib}^{5CI}$ (Ref. 20)	$\langle S(K)\rangle_{vib}^{IAM}$
1	0.7953	0.77	0.73	0.89
1.5	1.174	1.20	1.22	1.39
2	1.552	1.57	1.57	1.70
3	2.309	1.87	1.89	1.93
4	3.066	1.91	1.98	1.98
5	3.823	2.02	2.00	2.00
7	5.334	2.01	2.00	2.00
10	7.599	1.97	2.00	2.00

lighter elements.[10] A successful method of separately relating the elastic and inelastic differential cross sections to the chemical binding effects in molecules has also been established. Previous electron scattering determinations of binding effects[21,22] have relied on a single normalization of the observed cross section, in order to determine the intensity difference function, at $K > 40$ a.u. As shown in Ref. 10 it is essential that the utmost care must be taken to determine the proper background of scattered electrons to subtract from the observed intensity in order to put measurements for different scattering angles on the same intensity scale. Improper background corrections have been shown to result in 30% errors in the intensity multiplied by K^4 and hence considerably larger uncertainties may result in the intensity difference functions. We are not at this point claiming that the earlier work is incorrect; in fact for the case of H_2 the earlier work[21,22] is holding up amazingly well. The point to be made here is that the reliable determination of intensity difference functions by previous techniques either relied on photographic detection[21,22] with its inherent uncertainties, or electron counting of the total scattered intensity[23] which requires hours to record the data and hence the attainment of constant experimental conditions is more difficult to achieve. The present technique constitutes making a separate and independent experimental measurement for each data point in a time short compared to possible experimental fluctuations. Further it has been shown here and in Ref. 10 that the background problem can be solved in a way which eliminates the background almost completely as a source of experimental error. We feel that with an improved angular measurement capability, the approach used here to measure the intensity difference functions is superior in all respects to those so far employed.

*The authors wish to acknowledge support from the AFOSR Grant No. AFOSR-70-1900.
†Publication Number 2327 from the Chemical Laboratories of Indiana University.

[1]H. Bethe, Ann. Phys. (Leipz.) **5**, 325 (1930).
[2]M. Inokuti, Rev. Mod. Phys. **43**, 297 (1971).
[3]E. N. Lassettre, Can. J. Chem. **47**, 1733 (1969).
[4]J. Geiger, Z. Phys. **175**, 530 (1963).
[5]H. Schmoranzer, R. C. Ulsh, R. A. Bonham, and J. Ely, J. Chem. Phys. **57**, 1604 (1972).
[6]M. Inokuti and R. L. Platzman, in *Fourth International Conference on the Physics of Electronic and Atomic Collisions: Abstracts of Papers* (Science Bookcrafters, Hastings-on-Hudson, New York, 1965); p. 408; Argonne National Laboratory Report ANL-7060, p. 7, 1965.
[7]D. A. Kohl and L. S. Bartell, J. Chem. Phys. **51**, 2896 (1969).
[8]R. A. Bonham, J. Phys. Chem. **71**, 856 (1967).
[9]R. A. Bonham and C. Tavard, J. Chem. Phys. **59**, 4691 (1973).
[10]H. F. Wellenstein, R. A. Bonham, and R. C. Ulsh Phys. Rev. **A8**, 304 (1973).
[11]H. F. Wellenstein and R. A. Bonham Phys. Rev. **A7**, 1568 (1973).
[12]A. J. F. Metherell and M. J. Whelan, J. Appl. Phys. **37**, 1737 (1966), and H. F. Wellenstein, J. Appl. Phys. (to be published).
[13]R. A. Bonham and H. F. Wellenstein, J. Appl. Phys. **44**, 2631 (1973).
[14]A. Kollath, Ann. Phys. (Leipz.) **27**, 721 (1936).
[15]H. F. Wellenstein and R. E. Ensman, Rev. Sci. Instrum. **44**, 922 (1973).
[16]M. Blackman and J. L. Michiels, Proc. Phys. Soc. Lond. **60**, 549 (1948).
[17]P. Eisenberger, Phys. Rev. A **2**, 1678 (1970).
[18]R. E. Brown and V. H. Smith, Jr., Phys. Rev. A **5**, 140 (1972).
[19]A. L. Ford and J. C. Browne, Chem. Phys. Lett. **20**, 284 (1973).
[20]J. W. Liu, J. Chem. Phys. **59**, 1988 (1973).
[21]D. A. Kohl and R. A. Bonham, J. Chem. Phys. **47**, 1634 (1967).
[22]T. Iijima and R. A. Bonham, J. Phys. Chem. **67**, 2266 (1963).
[23]M. Fink and R. A. Bonham, J. Sci. Instrum. **41**, 389 (1970).